The Journal of Experimental Biology 212, 1876-1888
Published by The Company of Biologists 2009
doi:10.1242/jeb.030551

Division of labour and sex differences between fibrillar, tarsal adhesive pads in beetles: effective elastic modulus and attachment performance

James M. R. Bullock and Walter Federle*
Department of Zoology, University of Cambridge, Downing Street, Cambridge CB2 3EJ, UK
*Author for correspondence (e-mail: wf222@cam.ac.uk)

Accepted 19 March 2009

SUMMARY

Many beetles employ arrays of adhesive setae to control attachment during locomotion. Here we investigate whether and how variation in seta structure, both between sexes and between tarsal pads on the same leg, determines the mechanical properties and adhesive performance of fibrillar arrays. We vertically compressed individual adhesive pads to determine their effective elastic modulus. Distal adhesive arrays were significantly softer than middle and proximal ones. Variation in stiffness was mainly due to different seta diameters, but calculated elastic moduli of seta cuticle were relatively constant at 5–16 GPa. Consistent with their greater compliance, distal pads generated higher adhesion and friction on rough substrates. However, the greater stiffness of proximal pads conveys a superior ability to push. Proximal pads of males were less direction dependent than distal pads and generated larger pushing forces in the distal and lateral directions. In females, proximal pads also produced higher friction forces than distal pads, but only in the lateral direction. Video recordings of vertically climbing beetles confirmed that each pad was used differently. When legs above the body centre of gravity were pulling, beetles mainly engaged the distal pads, whereas legs below the centre of gravity mainly pushed with the proximal pads. Attachment performance was additionally compared between sexes on different substrates. Our findings demonstrate the presence of sex-specific specialisations of the fibrillar system as well as a division of labour between different adhesive pads on the same tarsus.

Key words: adhesion, biomechanics, locomotion, tribology.

INTRODUCTION

Many insects, spiders and lizards employ a fibrillar system of adhesion, consisting of dense arrays of microscopic adhesive setae. In insects alone, hairy adhesives have evolved at least three times independently (Beutel and Gorb, 2001) and the fibrillar morphology appears to represent a design optimized for dynamic attachment. Tarsal attachment pads not only have to adhere well on many different surface profiles but must also detach effortlessly during locomotion. Research into the fibrillar adhesive systems, both by biologists and engineers, has recently intensified, as it has become clear that they outperform conventional adhesives in several respects. For instance, they maximise adhesion *via* contact splitting (Arzt et al., 2003; Jagota and Bennison, 2002), adapt to different levels of surface roughness (Persson and Gorb, 2003), exhibit 'self-cleaning' properties (Hansen and Autumn, 2005), and offer dynamic adhesion, easily controllable through shear forces (Autumn et al., 2006a; Autumn and Hansen, 2006; Autumn et al., 2006b; Bullock et al., 2008; Federle, 2006).

The dock beetle *Gastrophysa viridula* De Geer (Chrysomelidae) has been investigated as a model organism for fibrillar adhesion (Bullock et al., 2008; Eimüller et al., 2008; Gorb, 2001; Peressadko and Gorb, 2004). It possesses three adhesive pads on the proximal three tarsal segments of each leg, which is a common feature in the superfamily Chrysomeloidea. These tarsal pads are morphologically distinct, and bear setae of different designs (Betz, 2003; Stork, 1980b; Stork and Evans, 1976; Voigt et al., 2008). Distal pads mainly contain spatula-tipped hairs, whereas proximal pads bear large numbers of hairs with simple, pointed tips. Furthermore, as for many other beetles, there is a conspicuous sexual dimorphism, with male-specific discoidal setae present in all three pads (though mainly in the first, proximal pad) (Pelletier and Smilowitz, 1987; Stork, 1980a; Stork, 1980b; Voigt et al., 2008). One consequence of this morphological diversity, observed in previous studies, is the fact that males produce stronger attachment forces (Pelletier and Smilowitz, 1987; Stork, 1980a; Voigt et al., 2008). However, the functional implications and adaptive value of the different seta and pad designs have remained largely unclear. Is each type of pad or seta optimised for a different function?

The different morphology of setae on the three tarsal segments suggests that they are specialised for different tasks. A division of labour between different attachment pads on the same foot has recently been found in cockroaches (Clemente and Federle, 2008). Here, the pretarsal arolium (at the foot tip) is used for pulling and generating adhesive forces, whereas the tarsal euplantulae are mainly used for pushing when the foot is pressed onto the surface, i.e. in a situation where no adhesion is needed. A similar specialisation for pushing and pulling appears to be present in spiders, where tarsal and pretarsal setae are morphologically specialised for pushing and pulling, respectively [tarsal setae bear microtrichia with spatula ends on the setal surface facing in the distal direction of the leg, whereas microtrichia are located on the opposite side in the pretarsal claw tuft setae (Hill, 1977; Niederegger and Gorb, 2006)].

However, no such obvious opposite orientation of setae appears to be present in leaf beetles. The distal adhesive pad of *G. viridula* is highly direction dependent, with friction forces towards the body greatly exceeding those away from it (Bullock et al., 2008). Direction-dependent attachment has also been observed in the fibrillar adhesive foot pads of geckos and flies (Autumn et al., 2006a; Autumn et al., 2000; Hill, 1977; Niederegger and Gorb, 2003), and

it is an important principle enabling rapid and efficient detachment during locomotion. The rapid control of attachment and detachment by shear forces is clearly beneficial for walking and running, but it has the possible adverse effect that legs are unable to push. Legs have to produce pushing forces both during walking on horizontal surfaces and during vertical climbing. It is unclear how beetles combine direction-dependent, controllable adhesion with the need to generate pushing forces, and whether the different morphologies of tarsal setae play any role in these processes.

To determine whether and how the three adhesive pads of leaf beetles (both male and female) are functionally different, we measured their stiffness as well as their adhesive and frictional performance. Similar to a previous study in geckos (Autumn et al., 2006c) we quantified the spring constants and effective elastic moduli of individual pads of live beetles using loading experiments. Friction and adhesion of single pads were measured in different directions as well as on rough and smooth surfaces. We address the following questions: (1) Do beetle adhesive pads differ in their mechanical properties? (2) Do pads differ in their ability to adhere to smooth and rough surfaces and in their direction dependence? (3) How are pads designed to resolve the conflict between effortless detachment and the need to generate pushing forces in the distal and lateral directions?

MATERIALS AND METHODS

Morphology of adhesive pads

The three adhesive pads of each sex of *Gastrophysa viridula* De Geer were imaged using scanning electron microscopy (SEM). Freshly amputated legs were fixed with 4% glutaraldehyde at 4°C for 24 h. Samples were washed with distilled water and gradually dehydrated using a series of increasing ethanol concentrations before critical point drying. To enable accurate measurements of seta width and length, some hairs were removed using the sharpened point of a fractured glass pipette. By ‘shaving’ the left half of the pad clean of hairs, side views of the medial, sagittal plane of the array were obtained. Samples were mounted on SEM stubs, sputter coated with 20 nm thick gold and studied with a FEI XL30-FEG at 2 or 5 kV.

Seta dimensions were measured from SEM images of side views of the medial and sagittal planes of the array, from one beetle of each sex, using custom MATLAB (The Mathworks, Natick, MA, USA) scripts. Hairs were measured at three equally spaced points along the proximal–distal axis (in the middle of the pad and at two points 50 µm proximal and distal from it). Seta diameter was measured in the middle of the setal shaft and seta tip width was measured at its widest point. Angles were measured in sagittal view relative to the horizontal plane of the pad. Lateral hair orientation was recorded in ventral view for each hair of the pad, as the absolute value of the angle relative to the proximal–distal axis. ‘Pad composition’ was calculated from the area of the pad occupied by one particular seta type and setal density (i.e. the number of setae per unit pad area) was obtained by manually counting the total number of hairs.

General set-up

G. viridula beetles were taken from laboratory colonies and weighed (body mass, males: 10.8±0.3 mg, females: 19.7±1.9 mg, means ± s.e.m.). As the material properties of arthropod cuticle are usually dependent on hydration (Vincent and Wegst, 2004) and excised tarsi can rapidly lose adhesion (Jiao et al., 2000), all experiments were performed with live insects. Beetles were mounted on a glass cylinder using Blu Tack and Parafilm tape as described in our prevous study (Bullock et al., 2008). The Blu Tack was used to fix one rear leg, isolating it and allowing the forces to be measured from each individual foot pad. This was achieved by aligning the pad parallel to the test substrate attached to the end of the force transducer (see Fig. 1). Additional Blu Tack was used to restrain the tarsus to prevent contact from neighbouring pads or claws.

The experimental setup allowed the measurement of single-pad adhesion and shear forces, as well as a simultaneous recording of contact area (Fig. 1). Forces were measured using a two-dimensional strain gage force transducer fixed to a three-axis motor positioning stage (M-126PD, Physik Instrumente, Karlsruhe, Germany). The motors were controlled with a custom LabVIEW (National Instruments, Austin, TX, USA) program which included a feedback mechanism allowing normal force to be kept constant. Voltage output was amplified (ME-Meßsysteme, Henningsdorf, Germany) and sampled at 1000 Hz with an I/O board (PCI-6035E, National Instruments). Foot pad forces were measured while in contact with a glass plate or other substrates (see below), attached to the transducer. On glass, ‘maximal setal’ contact area (the total real contact area of the hairs) was visualised with a coaxially-illuminated stereomicroscope (Federle et al., 2002). Images were recorded using a HotShot PCI 1280 B/W camera (NAC image technology, Simi Valley, CA, USA) and were analysed in MATLAB. A ‘projected’ pad area was also measured by manually drawing a polygon around the contact zone of the whole array, allowing values to be normalised for total pad area (Fig. 1).

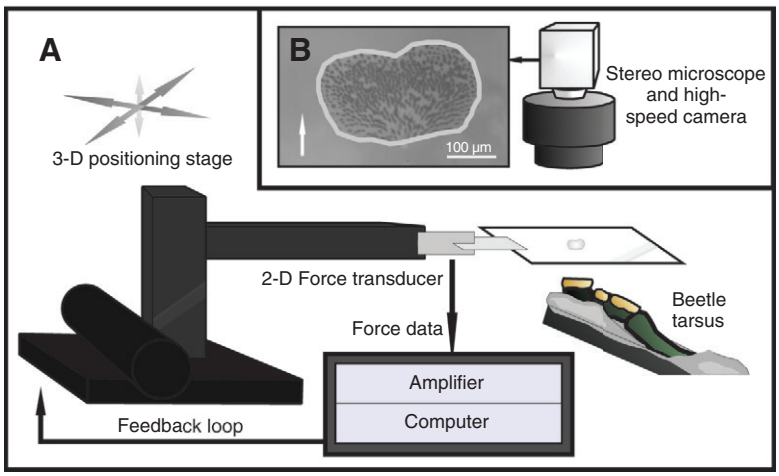

Fig. 1. (A) Experimental set-up for measuring single-pad friction, adhesion and contact area. (B) Contact area image. Arrow indicates the distal direction of the pad; the line polygon marks the projected contact area.

Pad spring constant and effective elastic modulus

In order to quantify the stiffness and effective elastic modulus of the adhesive pads of *G. viridula*, force–distance curves were recorded for small-strain compressions of each fibrillar pad. The glass plate of the force transducer was lowered into contact with each mounted pad for 10 s with a normal force feedback of 1.0 mN. The force feedback was then set to zero for 10 s, reducing the load so that the hairs were no longer compressed, but still in contact. The motor position in this situation was defined as the zero point for the displacement. The motors then compressed the pad by distances of 20 or 50 µm at a constant speed of 0.5 µm s^{-1}. To test for the presence of viscoelastic behaviour of the setal array, pads were left in compression for 2 min, and then the plate was withdrawn at the same velocity. We used a force transducer consisting of two cut plates of carbon-manganese steel joined at right angles to form a two-dimensional bending beam. Two mounted full bridges of 420 Ω semiconductor strain gauges (Micron Instruments, Simi Valley, CA, USA) allowed force measurement, calibrated as a function of lever arm length by applying milligram weights and defined displacements. The spring constant of the beam (at the position where measurements were taken) of 452 N m^{-1} was significantly higher than those obtained for each array (estimated from preliminary experiments) allowing small displacements of the fibrillar arrays to be investigated. Force–distance curves were recorded for all three pads of *G. viridula* hind legs (*N*=10 males, *N*=3 females). The projected contact area of the pad was simultaneously measured throughout the experiments to monitor the adhesive contact and to allow the spring constant to be normalised for area, giving the effective elastic modulus. Force data were filtered with a lowpass second-order Butterworth filter with sample frequency 100 Hz and cut-off frequency 0.25 Hz.

The recorded force–distance curves represent the behaviour of a system of springs in series, consisting of the force transducer, the setal array, the beetle's tarsal segment and the Blu Tack mounting material. The Blu Tack mount in our experiment behaved effectively as an incompressible solid so that its contribution could be safely neglected. This was confirmed with control tests where the above movement pattern was repeated with a small piece of glass in place of the beetle pad (the glass piece had approximately the same dimensions as the beetle tarsus, and was mounted in the same way). This showed a very high spring constant of approximately 4500 N m^{-1} for motor compressions of the Blu Tack bed. Blu Tack may exhibit some creep (Comyn, 1997) but this effect was found to be negligible within the range of normal forces in this experiment. The regression slope of the 20 µm compression experiments was used to measure the total spring constant k_{total}, from which the spring constant k_{pad} of each beetle pad was calculated:

$$k_{pad} = \frac{k_{beam} k_{total}}{k_{beam} - k_{total}} . \quad (1)$$

The effective elastic modulus of the setal array was calculated as:

$$E_{eff} = \frac{k_{pad} h}{A} , \quad (2)$$

where E_{eff} is the effective elastic modulus, k_{pad} the calculated spring constant, A the projected pad contact area and h the height of the array.

Two methods were used to model the bending-beam behaviour of the hairs; the full elastica cantilever model (Frisch-Fay, 1962) and the linear, small-strain cantilever model. From the equations presented in Autumn et al. (Autumn et al., 2006c) for the elastica model, we calculated the force *vs* displacement relationship for an oblique, cylindrical bending beam with radius r, length l, elastic modulus E and a range of angles θ to the horizontal. This was compared with the small-strain cantilever model, which (ignoring compression along the beam) predicts perpendicular displacement δ to be (Glassmaker et al., 2004; Persson, 2003; Sitti and Fearing, 2003):

$$\delta = \frac{4 l^3 F \cos^2\theta}{3\pi r^4 E} , \quad (3)$$

where F is the normal force per seta.

We estimated the elastic modulus of the seta cuticle from the measured force-displacement relationships for a ~20 µm compression of the different beetle pads and the dimensions of the setae. Values were initially calculated from the small-strain cantilever model (Eqn 3). As the strain was too large to be described satisfactorily by the small-strain model, we calculated correction factors from a linear regression to the first 20 µm of the full elastica model for the measured seta angle in each case.

Friction performance and direction-dependence

To investigate the direction dependence of attachment for all three pads of both sexes, shear movements were performed on a glass surface in the pulling, pushing and lateral directions. Pulling slides (corresponding to a movement of the leg towards the body) were performed at 500 µm s^{-1} over 10 mm with the force feedback employed to keep the load constant at 0.1 mN during the slide (*N*=5 beetles of each sex). Pushing slides (corresponding to a distal push of the leg away from the body) were additionally preceded by a short, 0.5 mm pulling movement to ensure proper contact of the hairs (*N*=5, both sexes). To investigate the effect of hair orientation, lateral (transverse) slides were performed as for the pull–push slides but with the pad rotated by first 90 deg. and then 270 deg. (*N*=2 beetles of each sex). At the end of every slide a 5 s pause was left before performing a 500 µm s^{-1} perpendicular pull-off to measure adhesion forces.

To test the attachment performance on a rough surface, we performed pulling and pushing slides (*N*=5 further beetles of each sex) on aluminium oxide polishing paper of 1 µm nominal asperity size (Ultra Tec, Santa Ana, CA, USA) glued to the glass coverslip on the force transducer. This particle size is smaller than the tips of the hairs, leading to reduced adhesive and frictional contact with the surface as shown in previous studies (Peressadko and Gorb, 2004; Voigt et al., 2008). The rough substrate prevented any recording of contact area. To estimate stresses, we used the mean values of maximal setal contact area recorded on glass. All slides were performed on a clean area of the substrate, and thus correspond to the 'little secretion' regime as described by Bullock et al. (Bullock et al., 2008). Sliding experiments were performed using a force transducer with a spring constant of 50 N m^{-1}, equipped with 350 Ω foil strain gauges.

Friction forces on female elytra

In addition to the slides recorded on smooth glass, friction and adhesion were measured for the proximal pads of male and female beetles on the smooth wing case of a female beetle (*N*=6 beetles of each sex). Wing cases were detached from just dead female beetles and glued to a coverslip attached to the force transducer. Pulling slides and pull-offs were performed as above although sliding velocity and distance were restricted to only 100 µm s^{-1} and 0.5 mm because of the limited length of the elytra. Pulling slides were performed in both directions along the length of the wing case so as to control for any directionality or anisotropy of the elytra surface,

and two repeats were taken for every slide. As for the rough surface slides, simultaneous area recordings could not be taken.

Locomotion recordings

In order to link our results on the function and performance of individual foot pads with whole insect locomotory behaviour, video recordings were taken of climbing beetles. Male and female beetles running up and down a smooth vertical surface were filmed in side view (N=16 runs from six beetles, with 145 steps analysed) with a HotShot PCI 1280 B/W high-speed video camera (NAC image technology, USA). The stance phase of each step (from front and rear legs) was analysed by recording the amount of time each pad (distal or proximal) remained in surface contact as a percentage of the total stance time. This 'relative pad contact time' provided a measure of how the pads are used during climbing.

RESULTS

Morphology of adhesive pads and setae

The tarsus of *G. viridula* consists of five segments and a distal pretarsus with the claws. The fourth segment is reduced and obscured by the third tarsomere. The proximal three tarsomeres bear on their ventral side adhesive pads, and will be referred to as 'proximal', 'middle' and 'distal' in this study. These pads are fibrillar arrays consisting of different seta types: spatula-tipped hairs, present on the distal-most tarsomere of both sexes, disk-tipped (discoidal) hairs, present on all pads of the male beetles only, and hairs with flattened and pointed tips, present in all pads (Fig. 2).

The distal-most pads of both sexes primarily contain thin, distally orientated spatula-tipped hairs, with a small number of pointed hairs around the edges. The males additionally have a cluster of discoidal hairs in the centre of the pad. The small middle pads are populated by pointed hairs, which point distally and laterally. A small number of discoidal hairs also exist on the middle pads of males. In the proximal pads there is the greatest sexual dimorphism. The female proximal pads are similar to the middle pads with pointed hairs that are oriented distally and laterally. The male pads, however, bear a large continuous field of discoidal hairs, fringed on the edges with pointed hairs (Fig. 2). In all pads, the hair tips form almost a perfect (horizontal) plane, meaning that hairs are slightly longer where the underlying pad cuticle curves away from the surface (Fig. 3). Array height was approximately 40 µm across all pads of both sexes, with the exception of male proximal pads, where the discoidal setae in the centre of the pad are considerably shorter and form a second plane set-in by ~15 µm from the longer pointed setae (see Fig. 3B).

From the side view images, both the pointed and the spatulate hairs appear to have a non-adhesive default position, with the seta tip contact zones oriented not only perpendicularly to the surface but even slightly away from it, so that the setal surface facing in the distal direction of the leg points towards the surface. This would imply that these hairs cannot be brought into contact with a simple perpendicular approach and that a small proximal shear (pull) should be needed [as observed for gecko setae (Autumn and Hansen, 2006)]. However, contact area imaging during the elastic modulus recordings showed that good contact was made by all hairs during a purely vertical compression. Hence, the extreme tip positions seen here may partly result from drying or preparation artefacts. By contrast, the tips of the discoidal hairs were aligned perfectly parallel with the substrate, suggesting that their default position is adhesive.

Spatula-tipped hairs (found on the distal pads of both sexes) were distinctly thinner (stalk diameter 1.4–1.5 µm) than middle and proximal pad hairs (diameters 2.2–2.6 µm). Measurements of mean lateral hair orientation (the absolute value of the angle relative to

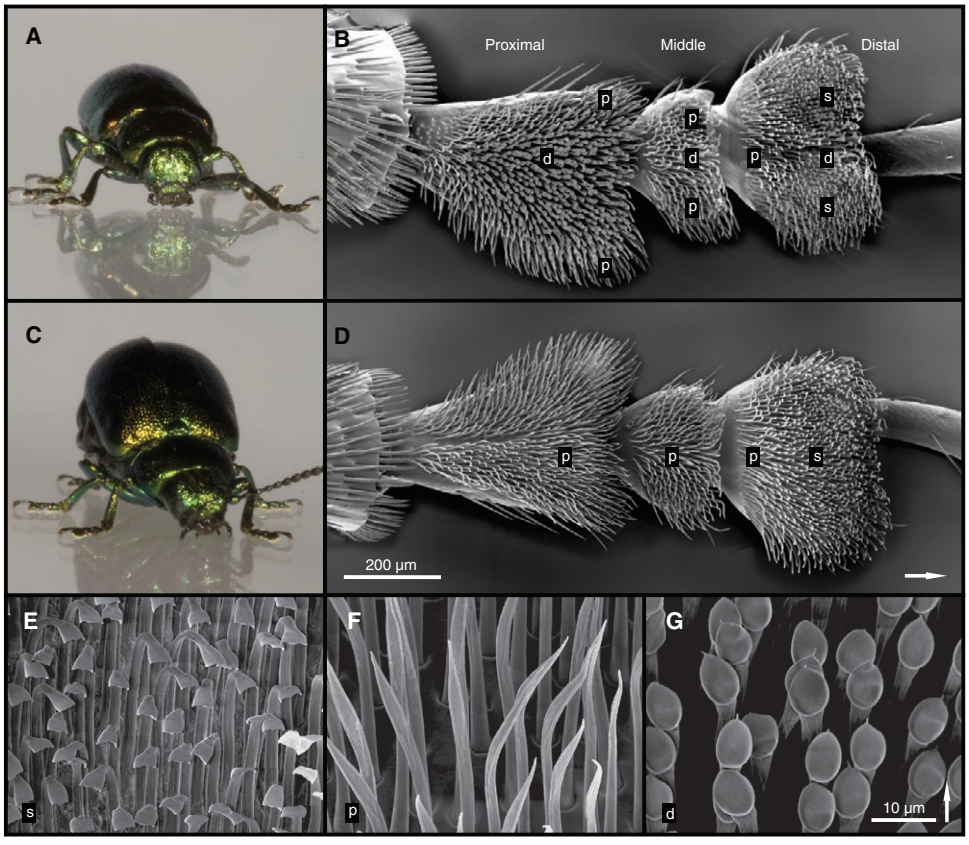

Fig. 2. Male (A,B) and female (C,D) dock beetles (*G. viridula*) and the attachment pads on their hind leg tarsus. E–G types of setae: spatula-tipped (E), pointed (F) and male-specific discoidal (G). Letters indicate hair type: s, spatula-tipped; p, pointed; d, discoidal. Arrows indicate distal direction. B,D and E,F,G, respectively, are of the same scale and orientation.

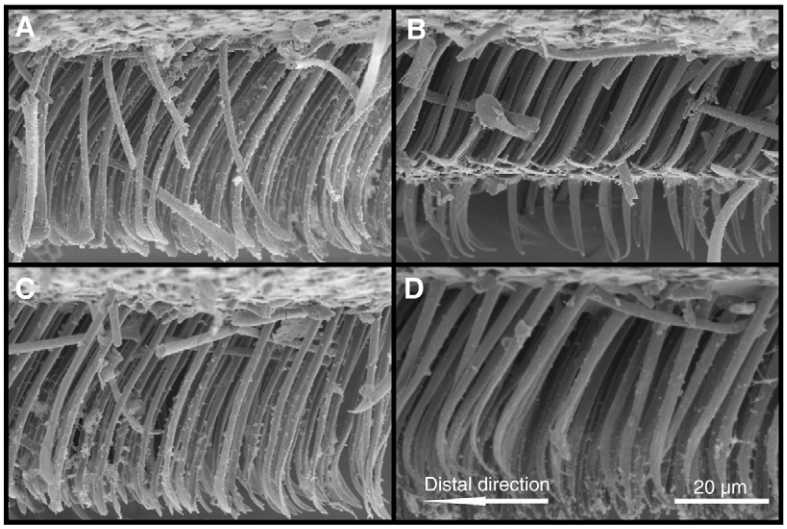

Fig. 3. Side views of adhesive pads in *G. viridula*. (A) Male distal pad,(B) male proximal pad, (C) female distal pad, (D) female proximal pad. Half the setae of the pad were shaved off to image setae in the medial plane of the pad. Note in the proximal pad of the male beetle (B) the two different planes formed by seta tips (discoidal setae shorter and pointed setae longer). The spatula-tipped setae of the distal pads (A,C) are visibly thinner than the discoidal and pointed setae on the other pads.

the proximal–distal axis of the pad in ventral view) showed that distal pads have hairs pointing mainly in the distal direction, whereas the middle pads of both sexes and the proximal pads of females have more laterally oriented hairs. The proximal pads of males are intermediate in this respect. Measurements of pad and seta properties are summarised in Table 1.

Pad spring constant and effective elastic modulus

To determine the material properties of the adhesive pads of *G. viridula*, we performed perpendicular compressions of the fibrillar arrays while simultaneously recording normal force and contact area. Two different compression depths were achieved with motor movements of 20 µm and 50 µm amplitude, resulting in actual seta tip displacements of 17.0±0.3 and 42.3±0.7 µm (mean ± s.e.m.). An example force trace is plotted in Fig. 4A,B. The large depth (50 µm, on the scale of the total array height) was chosen to characterize the compression behaviour of the system. The short depth (20 µm) was used to measure the array spring constant and effective elastic modulus.

During the 50 µm compression, forces increased non-linearly; with the slope initially decreasing (at ~15 µm) and then strongly increasing towards the end of the compression (see Fig. 4B). The initial decrease of the force-displacement slope may be explained by the similarly nonlinear shape exhibited by the full elastica cantilever model (Frisch-Fay, 1962) (see Fig. 4C). As the depth of the 50 µm compression exceeded the initial height of the setal array (approx. 40 µm), the setae will in this situation be pressed against the underlying tarsal cuticle, leading to a strong increase of the apparent stiffness. This was visible by the steep increase of forces when the motor displacement exceeded ~30 µm. Only a moderate decay of force (by 32.4±2.1% mean ± s.e.m.) was observed during the 2 min pause after the 20 µm motor compression. This indicates that beetle setae deformed largely elastically. Viscoelastic creep would be recognized by a decrease of the force over time as previously demonstrated for the smooth adhesive pads of bushcrickets (Gorb et al., 2000). The large force decay observed after the 50 µm motor compression suggests that in this situation, deformation occurred in another

Table 1. Morphological properties of the three tarsal adhesive pads in *G. viridula*

Sex	Pad	Seta type	Seta properties			Seta angle to horizontal (deg.)
			Array height (µm)	Hair diameter (µm)	Max. tip width (µm)	
Male	Distal	Spatula	37.5±1.1	1.4±0.1	4.1±0.4	49.7±2.1
	Middle	Pointed	38.6±0.8	2.2±0.2	2.2±0.3	45.3±3.6
	Proximal	Pointed	39.8±1.4	2.2±0.1	2.7±0.2	53.6±4.6
		Discoidal	25.7±0.3	2.3±0.1	6.0±0.6	58.3±1.0
Female	Distal	Spatula	38.1±1.6	1.5±0.0	3.8±0.3	57.0±2.4
	Middle	Pointed	42.2±2.5	2.2±0.1	2.5±0.1	54.8±1.7
	Proximal	Pointed	40.4±0.4	2.6±0.2	2.7±0.2	52.9±0.5

Sex	Pad	Approx. number of setae		Pad composition by seta type (%)			Lateral seta orientation [deviation (deg.) from proximal–distal axis]
		Total	Density (mm^{-2})	Spatula	Pointed	Discoidal	
Male	Distal	550	8500	77.6	10.3	12.1	8.2±0.5
	Middle	200	7500	0	95.8	4.2	45.0±3.3
	Proximal	700	8000	0	41.2	58.8	22.4±1.3
Female	Distal	650	9500	83.8	16.2	0	12.2±0.7
	Middle	150	5500	0	100	0	46.5±1.5
	Proximal	300	4500	0	100	0	52.2±1.2

Seta dimensions and angles (mean ± s.e.m.; *N*=3), measurements taken from one beetle of each sex.

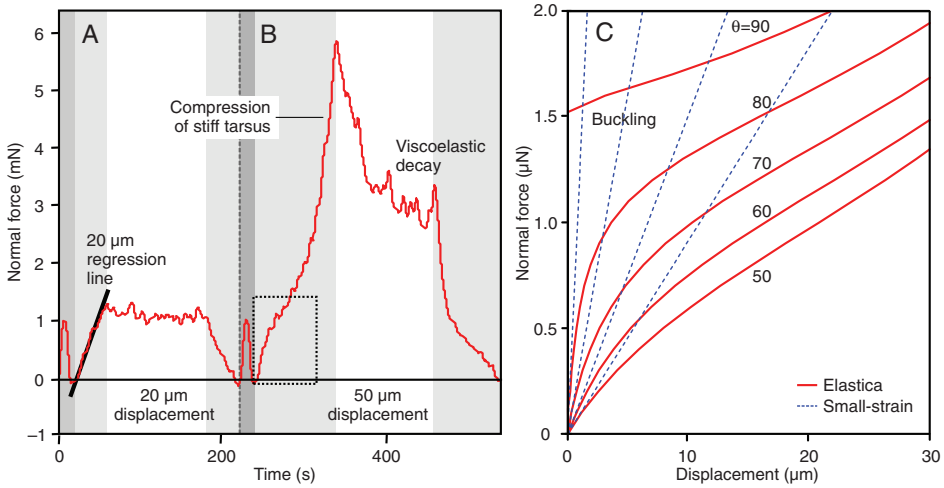

Fig. 4. Example force trace showing the compression of a distal adhesive pad of a female *G. viridula* beetle for 20 µm (A) and 50 µm (B) motor displacement. The slope of the regression line was used to calculate the spring constant of the setal array. Dark grey areas indicate the initial 1.0 mN loading and the return to the zero point *via* force feedback, light grey the compression, and white the 2 min pause before retraction. Viscoelastic decay is clearly visible in the 50 µm compression experiment. (C) Force–displacement relationship for a cylindrical cantilever beam with length 50 µm, radius 1 µm and elastic modulus 2 GPa, as predicted by the full elastica model (red) and small-strain model (blue) plotted for different angles. The shape of the initial part of the force-displacement curve (dashed box in B) was well predicted by the full elastica model, using the observed seta angles of between 40 deg. and 60 deg. (see Table 1).

component of the system that exhibits creep. The most probable explanation of this result is that the tarsus itself deforms viscoelastically.

From the results of the 20 µm compression, we calculated a first estimate of the elastic modulus of the seta cuticle using the small-strain cantilever model. From Eqn 3, the elastic modulus of a cylindrical hair of length 50 µm, radius 1 µm, angle 50 deg. and spring constant 0.1 N m^{-1} is estimated to be 2.27 GPa. Taking into account that for large strains, setae are less stiff than predicted by the small-strain model, we corrected these results with a factor derived from a linear regression of the first 20 µm compression of the full elastica prediction (Fig. 4C). Corrected cuticle elastic modulus values calculated for each pad are presented in Table 2; they varied only slightly between 5.2 and 16.1 GPa.

For both sexes, the spring constants of the proximal pads were significantly higher than those of the distal and middle pads (male; repeated measures ANOVA: F_2=36.492, P<0.001, Bonferroni-corrected paired *t*-tests for proximal *vs* distal: t_9=–7.332, P<0.001 and proximal *vs* middle: t_9=–6.185, P<0.001; Table 2, Fig. 5A). Unlike hemispherical smooth pads that increase contact area when pressed against a surface (Drechsler and Federle, 2006; Gorb et al., 2000), the beetle's planar fibrillar array showed little or no change in projected contact area during compression. Thus, a constant area was used for the calculation of the effective elastic modulus of the array. The effective elastic modulus of the proximal pads was still approximately twice as high as that of the distal pads. The smaller middle pads also had a high effective elastic modulus, significantly higher than that of the distal pads (repeated measures ANOVA: F_2=14.176, P<0.001; Bonferroni corrected paired *t*-test: proximal *vs* distal, t_9=–5.803, P<0.001; middle *vs* distal t_9=–4.929, P<0.001; Table 2, Fig. 5B).

Friction performance and direction dependence

To quantify the frictional and adhesive performance of the pads of male and female beetles, friction slides were performed on smooth and rough substrates, both along the leg and in the lateral direction. The results are summarized in Fig. 6 and Tables 3–5.

Smooth surface

Comparing between sexes, male beetles produced higher forces than females for friction slides on the smooth surface. This was most pronounced for pulls of proximal pads where males generated a 2.3 times greater friction than females (difference highly significant; see Table 3). Comparing between pads, the pulling forces of the (larger) proximal pads were similar to those of the distal pads, and in the case of the males, significantly larger (Table 3, Fig. 6). Steady sliding without any stick-slip was observed, in contrast to what has been proposed for the sliding of individual gecko spatulae (Yamaguchi et al., 2009).

Table 2. Spring constant, projected contact area and elastic modulus for proximal, middle and distal pads of male and female *G. viridula* beetles

	Male (*N*=10)			Female (*N*=3)		
Pad:	Distal	Middle	Proximal	Distal	Middle	Proximal
Spring constant (N m^{-1})	57.1±6.4	53.7±6.7	145.4±12.7	82.1±7.0	55.3±5.6	150.0±11.9
Projected contact area (µm^2)	65277±2802	26121±1737	87856±2169	66016±2512	27027±956	69692±4876
Effective elastic modulus (kPa)	34.2±3.2	81.1±9.5	65.1±5.4	53.6±6.1	88.0±10.5	92.3±5.5
Estimated cuticle modulus (GPa)	16.14	10.42	5.24	10.46	11.39	8.30

Values are mean ± s.e.m.

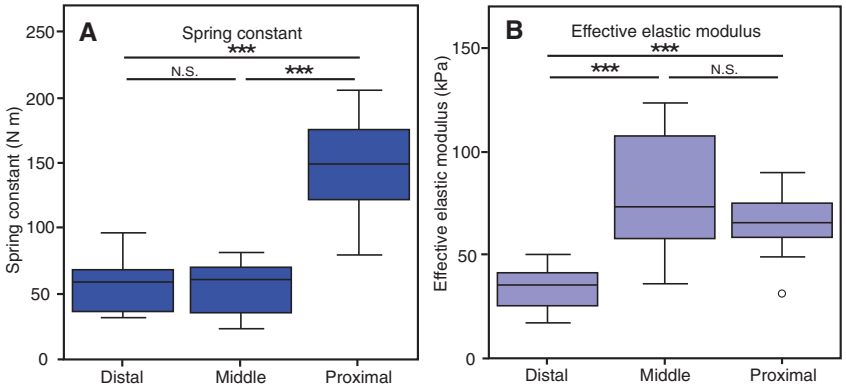

Fig. 5. Spring constant (A) and effective elastic modulus (B) data for all three pads of male beetles. *N*=10. Plot shows medians (centre lines), interquartile ranges (boxes), and the largest and smallest values (whiskers) that are not outliers (circles). Significance levels: **P*<0.05, ***P*<0.01, ****P*<0.001; N.S., not significant.

Rough surface

Presumably because of a lower real contact area on rough surfaces, forces were much lower than on the smooth substrate. This is consistent with findings from other studies comparing the effect of rough and smooth substrates on a fibrillar system (Voigt et al., 2008). An unsteady, macroscopic 'stick-slip' movement was observed, contrary to the steady sliding on the smooth substrate. On the rough surface, males no longer generated significantly higher forces, and females even produced significantly greater shear stress during pulls (Table 3, Fig. 6). Contrary to the smooth surface results, distal pads produced much higher forces than proximal pads (pulling friction: 3.5-fold in males, 3.1-fold in females; adhesion: 3.5-fold in males, 5.8-fold in females). Forces were higher despite the generally smaller size of distal pads, translating to an even larger difference in shear stress.

Friction forces on female elytra

The proximal pads of male and female beetles were tested on the fixed surface of a female wing case. No anisotropy of the elytra surface was found and no significant difference was seen for pulling slides up or down the elytra, in either males or females (male: friction t_5=–1.618, P=0.166, adhesion t_5=–1.952, P=0.108, female: friction t_5=0.108, P=0.918, adhesion t_5=0.513, P=0.630, paired t-tests). Therefore, data for pulling slides was pooled to test for significance

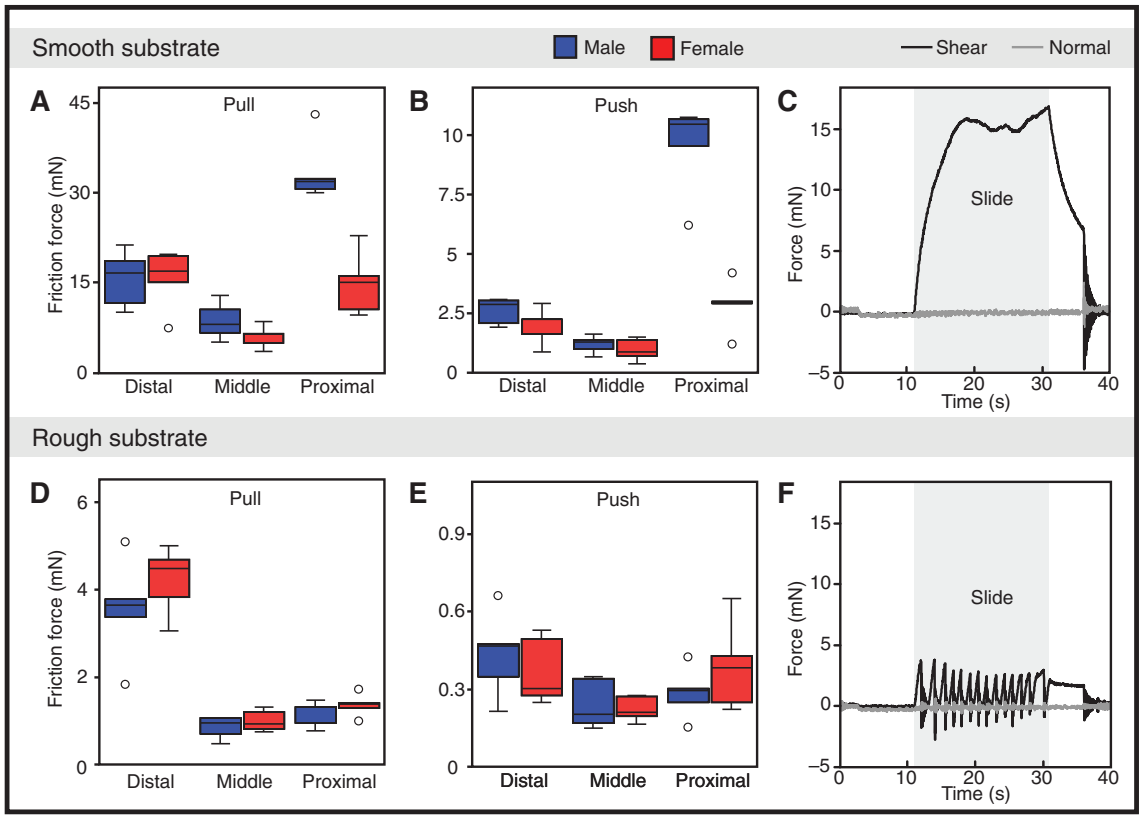

Fig. 6. Friction force measurements of *G. viridula* on smooth glass (A–C) and a rough, 1 μm grain polishing paper substrate (D–F). Values represent the peak force occurring during a 10 mm, 0.5 mm s^{-1} pulling (A,D) or pushing slide (B,E). *N*=5. Plots show medians (centre lines), interquartile ranges (boxes) and the largest and smallest values (whiskers) that are not outliers (circles). C and F show typical raw data curves for a pull of the distal pad of a female beetle on smooth (C) and rough (F) substrates. Shear (black) and normal (grey) forces are plotted. The grey shaded area indicates the 10 mm slide (0.1 mN normal force feedback), followed by a 5 s pause and 500 μm s^{-1} perpendicular pull-off, as described in Materials and methods.

Table 3. Friction force and shear stress for all pads of male and female beetles

Friction		Pad:	Male			Female		
			Distal	Middle	Proximal	Distal	Middle	Proximal
Smooth surface	Pull	Force (mN)	15.54±2.10	8.50±1.38	33.55±2.42	15.60±2.26	5.52±0.85	14.76±2.35
	(*N*=5)	Stress (kPa)	642±99	1088±219	1093±68	613±111	761±150	747±114
	Push	Force (mN)	2.58±0.25	1.18±0.16	9.51±0.85	1.84±0.34	0.95±0.21	2.84±0.48
	(*N*=5)	Stress (kPa)	203±18	535±172	585±92	144±38	413±162	589±177
Rough surface	Pull	Force (mN)	3.80±0.52	0.90±0.12	1.08±0.13	4.29±0.35	0.99±0.11	1.38±0.12
	(*N*=5)	Stress (kPa)	143±21	105±14	36±4	157±13	122±14	68±6
	Push	Force (mN)	0.43±0.07	0.24±0.04	0.29±0.04	0.37±0.06	0.22±0.02	0.39±0.08
	(*N*=5)	Stress (kPa)	26±4	57±10	14±2	21±3	62±6	46±9

Values are mean ± s.e.m. On the rough surface, contact area could not be measured therefore shear stress was calculated using the mean maximal setal contact area of the same pad on glass.

between sexes. As for the smooth surfaces, the proximal pads of the males produced much greater forces than those of the females during slides on the elytra (friction 3.9, adhesion 9.5 times greater; see Fig. 7). Sex differences were highly significant (friction: $t_{8.2}$=9.65, P<0.001; adhesion: $t_{7.8}$=6.00, P<0.001, unpaired t-tests). Owing to the shorter amplitude and smaller velocity, the forces on the elytra could not be directly compared with those measured on the other surfaces.

Direction-dependence of forces

Pulls, pushes and lateral slides were used to investigate the direction-dependence of the pads. We have previously recorded pulling and pushing slides in the distal pads of male *G. viridula* beetles (Bullock et al., 2008) and this is extended in the present study to include all three pads of both sexes. A strong direction-dependence was found for all pads of the beetles in all conditions (see Tables 3–5 and Fig. 6). However, it is important to note that for the proximal pads in males, this direction-dependence was weaker and relatively high forces were observed for pushing on a smooth surface. The higher stability of proximal pads in non-pulling directions was confirmed by lateral (transverse) slides (on the smooth surface, two beetles of each sex tested for all three pads), indicating stability in multiple directions. Proximal pads of both sexes appeared to support higher lateral friction (mean ± s.e.m., male, 11.85±2.73 mN; female, 6.50±1.18 mN) than the other pads, but forces were low (as for pushes) for the distal pads (males, 4.44±0.61 mN; females, 2.00±0.38 mN).

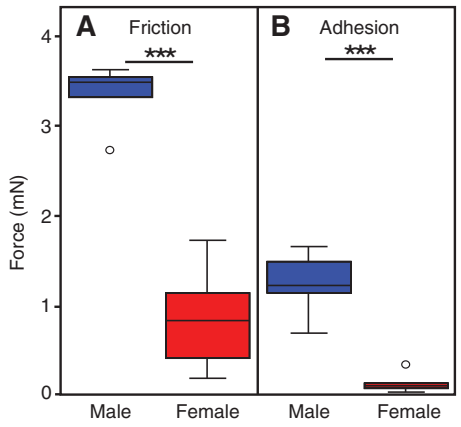

Fig. 7. Pulling slides (0.5 mm at 100 μm s^{-1}) of the proximal pads on a detached female elytra case. The comparison between males and females is presented for both friction forces (A) and adhesive forces (B). N=6. Plots show medians (centre lines), interquartile ranges (boxes) and the largest and smallest values (whiskers) that are not outliers (circles). Significance levels: *P<0.05, **P<0.01, ***P<0.001.

Use of adhesive pads during vertical climbing

We investigated the use of the three tarsal adhesive pads by filming male beetles climbing up a vertical smooth substrate. In most steps (N=43) all three segments appeared to be in contact with the surface. However, the selective use of proximal and distal adhesive pads was visible when pads did not remain in contact for the whole duration of the stance phase of the step (Fig. 8A–C). During upward walking, the front, 'pulling' legs were slammed firmly onto the surface and remained in contact until they peeled and detached from the proximal edge, the distal pads remaining in contact for almost the whole stance phase of the step (mean percentage of step time in contact ± s.e.m.: 98.2±0.6%). By contrast, proximal pads were little used and were in contact for less than half the stance phase of the step (mean: 43.6±3.0%). The proximal pads on the rear, 'pushing' legs, however, made almost continuous contact (mean: 98.1±1.2%), often slightly laterally oriented, whereas distal pads were lifted from the surface before the end of the step (mean: 42.5±4.2%).

During downwards walking all pads of the front legs were in contact for most of the stance phase of the step (N=47 steps). Contrary to the upwards climbing, the proximal pads appeared to be used almost continuously (mean: 85.7±2.5%). The rear leg distal pads were engaged almost exclusively (mean: 95.9±0.8%), with the proximal pads making hardly any contact (mean: 10.6±2.1%). At the end of the stance phase, the foot was detached from the distal edge and pulled along close to the surface.

This behaviour was also observed for female beetles (Fig. 8D–F), with the exception that both pads of the rear legs stayed in contact for most of the stance phase. This is probably explained by the additional mass that female beetles, heavily loaded with eggs, need to support (1.8 times that of the males). The large female beetles moved more slowly than the males, using a 'wave' rather than a 'tripod' gait. However, the distal pads were still in all cases employed during pulling and the proximal pads for pushing.

DISCUSSION

Our findings indicate that the fibrillar adhesive pads on the tarsal segments of *G. viridula* beetles have developed a functional division of labour similar to that recently reported for the smooth attachment pads of cockroaches (Clemente and Federle, 2008). The three adhesive pads of the same tarsus are not only composed of morphologically different types of setae, but also differ in their effective elastic modulus and adhesive/frictional performance.

Table 4. Adhesion and adhesive stress for all pads of male and female beetles (data corresponding to friction values presented in Table 3)

			Male			Female		
Adhesion		Pad:	Distal	Middle	Proximal	Distal	Middle	Proximal
Smooth surface	Pull	Force (mN)	2.25±0.66	0.52±0.14	4.24±0.34	1.30±0.31	0.29±0.10	1.01±0.34
	(*N*=5)	Stress (kPa)	100±27	68±18	142±11	53±10	53±21	55±18
	Push	Force (mN)	0.22±0.07	0.30±0.13	0.37±0.19	0.19±0.07	0.14±0.07	0.14±0.06
	(*N*=5)	Stress (kPa)	33±12	47±20	27±9	19±5	57±18	32±12
Rough surface	Pull	Force (mN)	0.49±0.17	0.14±0.04	0.13±0.02	0.69±0.10	0.09±0.03	0.12±0.04
	(*N*=5)	Stress (kPa)	20±7	18±5	4±1	26±4	11±3	6±2
	Push	Force (mN)	0.13±0.02	0.11±0.03	0.11±0.03	0.10±0.03	0.10±0.03	0.09±0.04
	(*N*=5)	Stress (kPa)	8±1	26±6	5±1	6±1	27±8	11±4

Values are mean ± s.e.m. Again, for the rough surface, area was estimated using the mean maximal setal contact area on glass.

Video recordings of freely walking beetles climbing upwards and downwards confirmed that proximal and distal pads are used differently and selectively during locomotion. Tarsi placed above the body centre of gravity mainly made contact using the distal pads, whereas feet below the centre of gravity primarily used their proximal pads. This suggests that the distal pads are mainly used for pulling and adhesion, whereas the proximal pads are used when legs have to push laterally or away from the body.

Direction dependence of tarsal adhesive pads

All three tarsal pads of *G. viridula* showed a clear direction-dependence, with forces being larger in the pulling than in the pushing direction. However, the stiffer proximal pads were less anisotropic and thus supported larger forces when pushed laterally or away from the body. The direction-dependence of many insect adhesive pads may be explained by the chain-like construction and flexibility of the tarsus (Snodgrass, 1935). Distal segments cannot exert large distal or lateral pushing forces, because the tarsus would easily buckle or bend (Clemente and Federle, 2008). By contrast, the proximal tarsus has greater stability and allows more distal and lateral pushing before buckling occurs. When the foot is pulled towards the body, a force on the distal adhesive pad will straighten the tarsus and align it to the force vector. If all three tarsal pads are in contact with the surface during a pulling stride, the peel force will be concentrated on the proximal pad, causing it to lift and detach from the surface earlier. The greater width of distal adhesive pads in many insects [e.g. bushcrickets (Beutel and Gorb, 2001), cockroaches (Clemente and Federle, 2008) and beetles (Stork, 1980b)] appears to support this function, as the peel force is proportional to pad width.

Direction-dependence of shear forces caused by tarsal buckling occurs in cockroaches [*Nauphoeta cinerea* (Clemente and Federle, 2008)] as well as stick insects and beetles (Bullock et al., 2008). However, the adhesive pads of both insects differ when tested ‘fixed’ (i.e. fully immobilized). While the fixed cockroach arolium and the euplantulae produced forces and shear stresses on a smooth surface that were similar during pushing and pulling (Clemente and Federle, 2008), all three tarsal pads in *G. viridula* showed higher forces in the pulling direction.

This direction-dependence on the level of the adhesive pad itself appears to be based on the fibrillar pad design and the asymmetrical structure of seta tips. Seta tips align with the

Table 5. Statistics comparing pulls of proximal and distal pads (for males and females), male and female beetles (for proximal pads only as no significant differences are found between sexes for distal pads) and pulls and pushes

			Smooth		Rough	
Proximal *vs* distal pads (paired *t*-test)	Males	Friction slides	t_4=–4.753	*P*=0.009	t_4=4.897	*P*=0.008
		Shear stress	t_4=–3.939	*P*=0.017	t_4=5.317	*P*=0.006
		Adhesion	t_4=–2.719	*P*=0.053	t_4=2.132	*P*=0.100
		Adhesive stress	t_4=–1.599	*P*=0.185	t_4=2.272	*P*=0.086
	Females	Friction slides	t_4=0.283	*P*=0.791	t_4=8.746	*P*<0.001
		Shear stress	t_4=–2.400	*P*=0.074	t_4=7.385	*P*=0.002
		Adhesion	t_4=0.733	*P*=0.504	t_4=6.437	*P*=0.003
		Adhesive stress	t_4=–0.123	*P*=0.908	t_4=6.220	*P*=0.003
Males *vs* females proximal pads (unpaired *t*-test)		Friction slides	$t_{8.0}$=5.575	*P*<0.001	$t_{7.9}$=–1.542	*P*=0.162
		Shear stress	$t_{6.5}$=2.613	*P*=0.037	$t_{7.3}$=–4.470	*P*=0.003
		Adhesion	$t_{8.0}$=6.725	*P*<0.001	$t_{5.6}$=0.030	*P*=0.977
		Adhesive stress	$t_{6.5}$=4.131	*P*=0.005	$t_{4.7}$=–1.145	*P*=0.307

		Males					
Pushing *vs* pullling friction force (paired *t*-test)	Pad	Distal		Middle		Proximal	
	Smooth	t_4=6.163	*P*=0.004	t_4=5.280	*P*=0.006	t_4=10.084	*P*<0.001
	Rough	t_4=5.598	*P*=0.005	t_4=4.313	*P*=0.013	t_4=5.763	*P*=0.004
		Females					
	Pad	Distal		Middle		Proximal	
	Smooth	t_4=6.717	*P*=0.003	t_4=6.288	*P*=0.003	t_4=5.142	*P*=0.007
	Rough	t_4=10.646	*P*<0.001	t_4=6.505	*P*=0.003	t_4=8.689	*P*<0.001

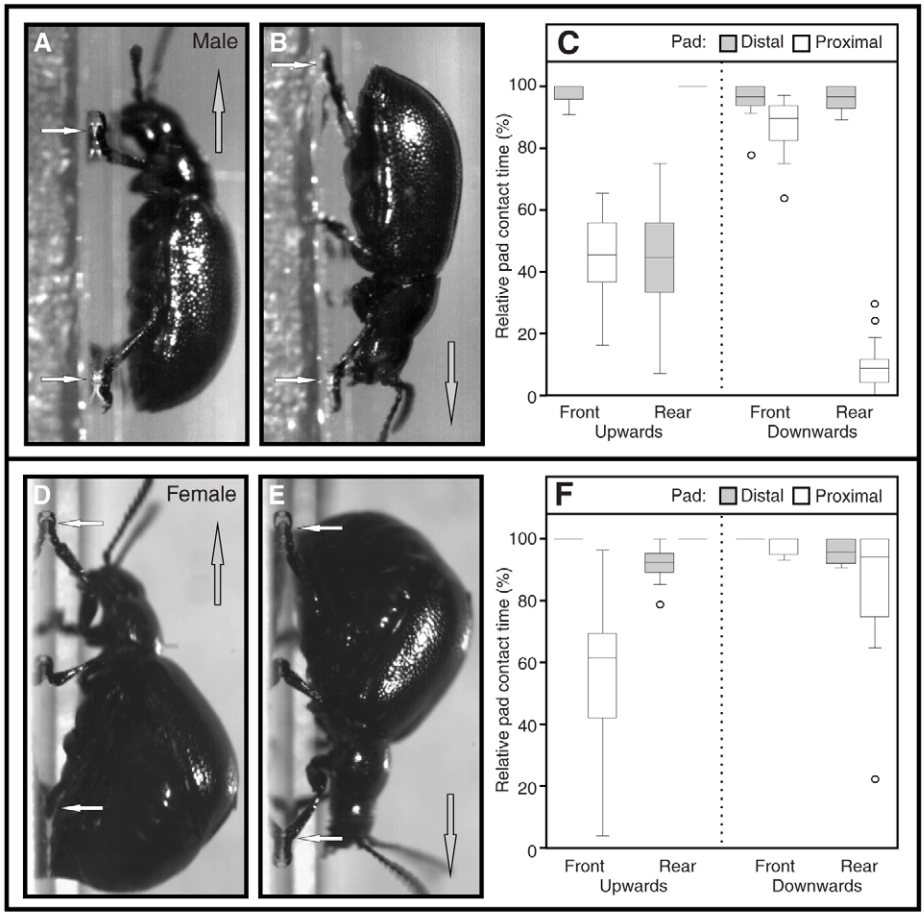

Fig. 8. *G. viridula* male (A,B) and female (D,E) beetles climbing up (A,D) and down (B,E) a smooth vertical surface. The white arrows indicate pads contacting the surface (upwards: the distal pad for the front, 'pulling' leg and the proximal pad for the rear, 'pushing' leg; downwards: both pads for the front leg, the distal pad for the rear leg). (C,F) Boxplots showing the percentage time each pad (distal, grey; proximal, white) remained in contact with the surface, relative to the total duration of the stance phase of the step for male (C) and female (F) beetles. Results presented for front and rear legs, as well as upwards and downwards climbing.

substrate when the pad is pulled. When pads are strongly pushed away from the body, setae deflect so that their tips are no longer able to align with the substrate. In many cases, the unstressed default orientation of seta tips is non-adhesive, so that they require a pull towards the body to become aligned (Autumn et al., 2006a; Autumn and Hansen, 2006; Federle, 2006). It is probable that this non-adhesive default state results in a particularly effortless, 'automatic' detachment as soon as the shear force towards the body is released. Interestingly, Fig. 3 suggests that only the pointed and spatulate setae in *G. viridula* have this non-adhesive default position and this may explain the weaker direction-dependence of the proximal pads in males. In general, direction-dependence of adhesive pads allows animals to switch easily and rapidly between attachment and detachment by performing gross leg movements toward the body or away from it. Our findings suggest that the detachment of the proximal pads in *G. viridula* should be more cumbersome, but more detailed observations of tarsal movements in freely walking beetles and of ground reaction forces are needed to test this prediction.

When viewed from the ventral side, the spatula-tipped hairs of the beetle's distal pad are more exactly aligned in the proximal–distal direction than those of the proximal pad. This orientation may also be responsible for the clearer direction-dependence of distal pads, with strong 'pulling' forces (when setae are loaded in tension) and easy detachment when 'pushing' (where setae are compressed along their axis) (Bullock et al., 2008). By contrast, setae on the proximal pads were oriented more transversely and consistently, proximal pads were able to produce higher lateral forces (in both sexes) and, at least for the males, higher pushing forces.

Although force vectors typically point along the legs to minimise torques about the joints (Full et al., 1991), lateral forces may be important in some situations, for example in middle or hind legs during climbing (Goldman et al., 2006). In the lateral sliding tests, at least half of the pointed hairs (those on the side opposite to the sliding direction) may be able to contact the surface in tension, corresponding to substantial frictional and adhesive forces. This may provide a way to push laterally without sacrificing direction-dependent detachment (Fig. 9).

Specialisation of attachment pads for pushing and pulling (as in cockroaches and spiders) may correlate with a specialisation for friction and adhesion, respectively. To be able to climb on natural surfaces, which usually exhibit some degree of surface roughness, insects might have evolved more compliant pads, allowing them to conform better to the surface profile. The fibrillar design is inherently well suited for this purpose for several reasons. Firstly, long and flexible setae bend easily so that their tips can make contact with an irregular substrate without the need for high normal forces. Secondly, the small size of seta tips makes fibrillar pads insensitive to roughness at a larger length scale. Lastly, contact to even smaller length scales of surface roughness may be facilitated by the bending of spatula tips, which are usually very thin (Eimüller et al., 2008; Persson and Gorb, 2003).

However, enhanced compliance may come at a cost, because soft adhesive pads will be more susceptible to wear, in particular when softer materials are used. Pads of climbing animals have to resist considerable shear forces over many steps in an entire lifetime. Abrasion and wear probably represent a significant problem for soft attachment pads (e.g. Ridgel et al., 2003; Slifer, 1950), calling for

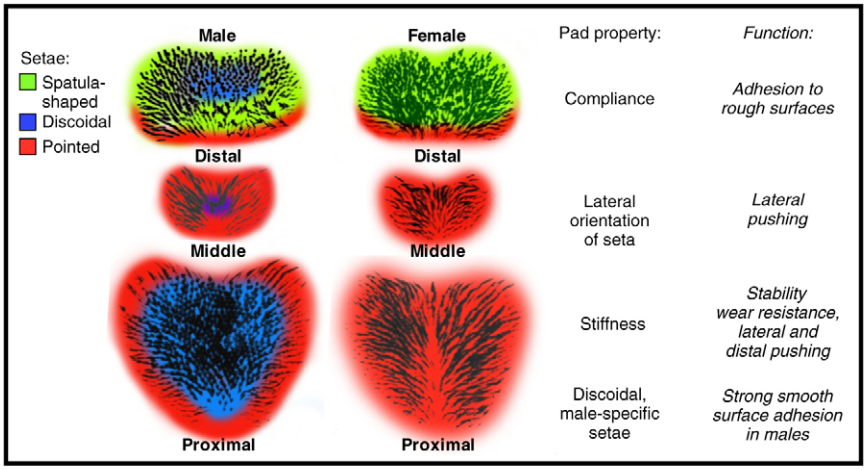

Fig. 9. Summary of the proposed functional properties for each pad (distal, middle and proximal) of both sexes of *G. viridula*. Epi-illumination contact area images; colours mark the position of the different seta types.

a more robust and thus less compliant pad design. Fibrillar adhesive systems are to some extent able to achieve compliance with relatively stiff and wear-resistant materials, but here too compliance may be limited by the condensation or 'self-matting' of hairs (Glassmaker et al., 2004; Persson, 2003; Sitti and Fearing, 2003; Spolenak et al., 2005). If pads are primarily used under compression to generate friction forces, wear resistance will be even more critical but the requirement for compliance may be relaxed, because on rough substrates high friction forces can be achieved by interlocking even with little adhesion. Stiffer proximal pads may also provide better stability when compressed by the insect's body weight. If the beetle was walking only on its distal pads (with three legs in contact at any one time), the setae would be deflected by 0.64 µm for males and 0.82 µm for females. Although this is small and well within the elastic range of the hairs, support from stiffer proximal pads may prove beneficial for situations with additional loads. Thus, a division of labour between soft, adhesive pads and more robust and wear-resistant friction pads may evolve as a consequence of a trade-off between compliance and wear resistance. The occurrence of a similar division of labour between proximal and distal tarsal pads in beetles (this study), cockroaches (Clemente and Federle, 2008) and presumably spiders (Hill, 1977; Niederegger and Gorb, 2006) suggests that this is a fundamental principle, widespread among arthropods.

Array stiffness and performance on rough surfaces

Our measurements of the effective elastic modulus of individual adhesive pads in *G. viridula* show that the distal pads of *G. viridula* are about twice as compliant as the middle and proximal pads. This difference in stiffness supports the observed functional division of labour between adhesive pads on the same foot. Greater compliance enhances the ability of a pad to adapt to rough substrates. Consistently, on the rough substrate we measured three to five times higher forces and stresses for the smaller, yet softer, distal pads than for the proximal pads in both males and females.

The adhesive and frictional performance of the different tarsal pads in *G. viridula* is based both on the structure of the seta tips and on the compliance of seta stalks. For large deformations, array stiffness is mainly affected by the bending of seta stalks. Seta bending is thus responsible for the ability of pads to conform to large-scale surface roughness. On a smaller length scale, adhesion will be mainly determined by the geometry, size and material properties of the seta tips. The higher compliance of the distal pads coincides with a primarily spatulate tip design. The spatulae are very thin and thus ensure a high flexibility that can compensate small-scale surface roughness (Persson and Gorb, 2003). To enable adhesion to natural surfaces with many length scales of surface roughness, a combination of seta stalk compliance and flexible tips is required, and this explains why both features are present in distal pads of beetles.

It should be noted that during free walking on a rough surface, other parts of the tarsus and pretarsus may be used. In all insects, the pretarsal claws contribute to pulling (Dai et al., 2002) and many insects (including *G. viridula*) have distally oriented, stiff spines on the tibia (near the tibia–tarsus joint), which regularly contact the ground and are probably used for pushing [e.g. froghoppers (Burrows, 2006)].

Despite the variation in stiffness, all three pads of *G. viridula* were so compliant that their effective elastic moduli fell within Dahlquist's criterion for tack (E_{eff}<100 kPa) (Dahlquist, 1969). This empirical criterion was introduced for bulk adhesive materials. For fibrillar adhesives, however, this condition is necessary but not sufficient for good adhesion, as the adhesive contact also depends on the geometry of the seta tips, which can vary independently of the effective elastic modulus of the array. The values measured here for *G. viridula* are close to results obtained for gecko fibrillar arrays [E_{eff}=83±4.0 kPa (Autumn et al., 2006c)].

Material properties of seta cuticle

Using the measured pad spring constants, we estimated the elastic modulus of the seta cuticle to range from 5.2–16.1 GPa. This is slightly higher than the range estimated by Orso et al. (Orso et al., 2006) for a hydrated seta (2–6 GPa) but is consistent with their figure calculated from tensile tests of a dried seta, of 13.3±1.0 GPa. Although this comparison between elastic modulus values measured in a tensile and a bending test may have limited validity, it suggests that the stiffness of a hydrated seta is not very different from that of a dried one. This indicates that the seta cuticle is quite hydrophobic and may contain little water *in vivo*.

A similar effect has been reported for locust wings, where the cuticle of the thin wing membrane was found to be unusually insensitive to hydration (Smith et al., 2000). Being unaffected by (de-)hydration may also be biologically advantageous in an adhesive system, because setae may be particularly exposed to the environment and to a wide range of humidity conditions. The elastic modulus we measured is strikingly high, and is in fact close to the highest values ever reported for insect cuticle [20 GPa measured in the locust tibia (Ker, 1977; Vincent and Wegst, 2004)]. A high elastic

modulus of the cuticle making up the adhesive pad may provide increased wear resistance during repeated steps. It should be noted that in addition to bending, setae may also deflect by rotating in their socket, i.e. the hair socket could act as a hinge. This would result in an even higher predicted value for the cuticle modulus. Further work is needed to investigate whether adhesive seta cuticle is indeed less hydration dependent than other types of insect cuticle and if so, how this property relates to the chemical composition of the cuticle.

The calculated Young's modulus of seta cuticle varied only little between pads. Instead, the greater compliance of the distal pad appears to be achieved mainly by thinner seta stalks. This may be the simplest and most effective way to increase seta compliance, because seta radius appears to the fourth power in Eqn 3. Hence, a small decrease in hair thickness will strongly reduce the effective elastic modulus of the array. The same change would require a much larger relative change of cuticle modulus, and although cuticle may be a highly variable material (Vincent and Wegst, 2004), a strong hydration dependence is undesirable as discussed above. Interestingly, the elastic modulus of the gecko's setal β-keratin also appears to be relatively conserved across species (at approximately 1.5 GPa), again implying a reliance on morphological parameters rather than material properties (Peattie et al., 2007). The hydration dependence of gecko seta material has not been investigated but the elastic modulus of avian keratin is also only moderately dependent on humidity (Taylor et al., 2004).

Sex specific differences of attachment

Beetle seta design does not only differ between different tarsal segments of the same foot but also between sexes. The wide-spread sexual dimorphism can be explained by the need of males to maintain a firm and long-lasting hold on the relatively smooth elytra of females during copulation. An adhesive system adapted to generate large forces on smooth surfaces is clearly advantageous for this purpose (Pelletier and Smilowitz, 1987; Stork, 1980a; Voigt et al., 2008). As a consequence of sexual conflict, females of diving beetles have evolved surface corrugations on their elytra that make it more difficult for males to adhere, triggering further modifications of the male adhesive system (Bergsten et al., 2001) but no such effects are presently known for leaf beetles.

In this study we confirmed the stronger adhesion of males to female elytra and smooth surfaces on the level of individual pads. Consistent with the setal composition, the greatest difference in forces on a smooth surface was found for the proximal pads which possess many discoidal setae in males but not in females. On smooth glass, males were able to generate over twice the friction force of the females (or 1.5 times the shear stress) and an even stronger difference was found for the friction produced on female elytra. This confirms the important role of discoidal setae on male proximal pads in the attachment to the smooth surface of females during mating.

The absence of discoidal setae in the proximal pads of females suggests that their presence might entail a cost for males. Firstly, male proximal pads achieved slightly smaller shear forces and stresses than female ones on the rough surface (see also Voigt et al., 2008). Secondly, the weaker direction-dependence of male proximal pads might make it more difficult for the pads to detach rapidly from a smooth surface.

Outlook

Despite a large number of recent studies and efforts to 'mimic' biological fibrillar adhesives (for a review, see del Campo and Arzt, 2007), very little is actually still known about the properties and the performance of the natural systems. In fact many synthetic adhesives do not fall within the parameter space of biological adhesives (with respect to size and stiffness of setae) and their performance often falls short of the natural systems. This may be partly due to a lack of understanding of the biological systems which are being imitated. Apart from recent work on beetles and geckos (Orso et al., 2006; Peattie et al., 2007), only limited information is available on the material properties of adhesive setae. For many systems, the frictional and adhesive performance is unknown, making it impossible to test available theoretical models. Analyzing the material properties of natural adhesive pads as well as their adhesive performance and locomotion represents an essential step towards the development of biomimetic fibrillar adhesives.

We wish to thank Andreas Eckart, Patrick Drechsler and Filip Szufnarowski for their help in the development of the LabVIEW motor control programmes. This study was funded by research grants from the Deutsche Forschungsgemeinschaft (Emmy-Noether Fellowship FE 547/1 to W.F.), the UK Biotechnology and Biological Sciences Research Council and the Cambridge Isaac Newton Trust.

REFERENCES

Arzt, E., Gorb, S. and Spolenak, R. (2003). From micro to nano contacts in biological attachment devices. *Proc. Natl. Acad. Sci. USA* **100**, 10603-10606.
Autumn, K. and Hansen, W. (2006). Ultrahydrophobicity indicates a non-adhesive default state in gecko setae. *J. Comp. Physiol. A* **192**, 1205-1212.
Autumn, K., Liang, Y. A., Hsieh, S. T., Zesch, W., Chan, W. P., Kenny, T. W., Fearing, R. and Full, R. J. (2000). Adhesive force of a single gecko foot-hair. *Nature* **405**, 681-685.
Autumn, K., Dittmore, A., Santos, D., Spenko, M. and Cutkosky, M. (2006a). Frictional adhesion: a new angle on gecko attachment. *J. Exp. Biol.* **209**, 3569-3579.
Autumn, K., Hsieh, S. T., Dudek, D. M., Chen, J., Chitaphan, C. and Full, R. J. (2006b). Dynamics of geckos running vertically. *J. Exp. Biol.* **209**, 260-272.
Autumn, K., Majidi, C., Groff, R. E., Dittmore, A. and Fearing, R. (2006c). Effective elastic modulus of isolated gecko setal arrays. *J. Exp. Biol.* **209**, 3558-3568.
Bergsten, J., Toyra, A. and Nilsson, A. N. (2001). Intraspecific variation and intersexual correlation in secondary sexual characters of three diving beetles (Coleoptera: Dytiscidae). *Biol. J. Linn. Soc.* **73**, 221-232.
Betz, O. (2003). Structure of the tarsi in some *Stenus* species (Coleoptera, Staphylinidae): external morphology, ultrastructure, and tarsal secretion. *J. Morphol.* **255**, 24-43.
Beutel, R. G. and Gorb, S. N. (2001). Ultrastructure of attachment specializations of hexapods (Arthropoda): evolutionary patterns inferred from a revised ordinal phylogeny. *J. Zool. Syst. Evol. Res.* **39**, 177-207.
Bullock, J. M. R., Drechsler, P. and Federle, W. (2008). Comparison of smooth and hairy attachment pads in insects: friction, adhesion and mechanisms for direction-dependence. *J. Exp. Biol.* **211**, 3333-3343.
Burrows, M. (2006). Morphology and action of the hind leg joints controlling jumping in froghopper insects. *J. Exp. Biol.* **209**, 4622-4637.
Clemente, C. J. and Federle, W. (2008). Pushing *versus* pulling: division of labour between tarsal attachment pads in cockroaches. *Proc. Biol. Sci.* **275**, 1329-1336.
Comyn, J. (1997). *Adhesion Science*. Cambridge: Royal Society of Chemistry.
Dahlquist, C. A. (1969). *Treatise on Adhesion and Adhesives*, vol. 2 (ed. R. L. Patrick), pp. 219-260. New York: Marcel Dekker.
Dai, Z., Gorb, S. N. and Schwarz, U. (2002). Roughness-dependent friction force of the tarsal claw system in the beetle *Pachnoda marginata* (Coleoptera, Scarabaeidae). *J. Exp. Biol.* **205**, 2479-2488.
del Campo, A. and Arzt, E. (2007). Design parameters and current fabrication approaches for developing bioinspired dry adhesives. *Macromol. Biosci.* **7**, 118-127.
Drechsler, P. and Federle, W. (2006). Biomechanics of smooth adhesive pads in insects: Influence of tarsal secretion on attachment performance. *J. Comp. Physiol. A* **192**, 1213-1222.
Eimüller, T., Guttmann, P. and Gorb, S. N. (2008). Terminal contact elements of insect attachment devices studied by transmission X-ray microscopy. *J. Exp. Biol.* **211**, 1958-1963.
Federle, W. (2006). Why are so many adhesive pads hairy? *J. Exp. Biol.* **209**, 2611-2621.
Federle, W., Riehle, M., Curtis, A. S. G. and Full, R. J. (2002). An integrative study of insect adhesion: mechanics and wet adhesion of pretarsal pads in ants. *Integr. Comp. Biol.* **42**, 1100-1106.
Frisch-Fay, R. (1962). *Flexible Bars*. London: Butterworths.
Full, R. J., Blickhan, R. and Ting, L. H. (1991). Leg design in hexapedal runners. *J. Exp. Biol.* **158**, 369-390.
Glassmaker, N. J., Jagota, A., Hui, C. Y. and Kim, J. (2004). Design of biomimetic fibrillar interfaces. 1. Making contact. *J. R. Soc. Interface* **1**, 23-33.
Goldman, D. I., Chen, T. S., Dudek, D. M. and Full, R. J. (2006). Dynamics of rapid vertical climbing in cockroaches reveals a template. *J. Exp. Biol.* **209**, 2990-3000.
Gorb, S. N. (2001). *Attachment Devices of Insect Cuticle*. Boston, MA: Kluwer Academic Publishers.

Gorb, S., Jiao, Y. and Scherge, M. (2000). Ultrastructural architecture and mechanical properties of attachment pads in *Tettigonia viridissima* (Orthoptera Tettigoniidae). *J. Comp. Physiol. A* **186**, 821-831.
Hansen, W. R. and Autumn, K. (2005). Evidence for self-cleaning in gecko setae. *Proc. Natl. Acad. Sci. USA* **102**, 385-389.
Hill, D. E. (1977). The pretarsus of salticid spiders. *Zool. J. Linn. Soc.* **60**, 319-338.
Jagota, A. and Bennison, S. J. (2002). Mechanics of adhesion through a fibrillar microstructure. *Integr. Comp. Biol.* **42**, 1140-1145.
Jiao, Y., Gorb, S. and Scherge, M. (2000). Adhesion measured on the attachment pads of *Tettigonia viridissima* (Orthoptera, Insecta). *J. Exp. Biol.* **203**, 1887-1895.
Ker, R. F. (1977). *Some Structural and Mechanical Properties of Locust and Beetle Cuticle*. D Phil. Thesis: University of Oxford.
Niederegger, S. and Gorb, S. (2003). Tarsal movements in flies during leg attachment and detachment on a smooth substrate. *J. Insect Physiol.* **49**, 611-620.
Niederegger, S. and Gorb, S. N. (2006). Friction and adhesion in the tarsal and metatarsal scopulae of spiders. *J. Comp. Physiol. A* **192**, 1223-1232.
Orso, S., Wegst, U. G. K., Eberl, C. and Arzt, E. (2006). Micrometer-scale tensile testing of biological attachment devices. *Adv. Mater.* **18**, 874-877.
Peattie, A. M., Majidi, C., Corder, A. and Full, R. J. (2007). Ancestrally high elastic modulus of gecko setal β-keratin. *J. R. Soc. Interface* **3**, 1071-1076.
Pelletier, Y. and Smilowitz, Z. (1987). Specialized tarsal hairs on adult male Colorado potato beetles, *Leptinotarsa decemlineata* (Say), hamper its locomotion on smooth surfaces. *Can. Entomol.* **119**, 1139-1142.
Peressadko, A. G. and Gorb, S. N. (2004). Surface profile and friction force generated by insects. In *First International Industrial Conference Bionik 2004, Fortschritt-Berichte VDI 15, Nr. 249* (ed. I. Boblan and R. Bannasch), pp. 257-263. Düsseldorf: VDI Verlag.
Persson, B. N. J. (2003). On the mechanism of adhesion in biological systems. *J. Adhes. Sci. Technol.* **118**, 7614-7620.
Persson, B. N. J. and Gorb, S. (2003). The effect of surface roughness on the adhesion of elastic plates with application to biological systems. *J. Chem. Phys.* **119**, 11437-11444.
Ridgel, A. L., Ritzmann, R. E. and Schaefer, P. L. (2003). Effects of aging on behavior and leg kinematics during locomotion in two species of cockroach. *J. Exp. Biol.* **206**, 4453-4465.
Sitti, M. and Fearing, R. S. (2003). Synthetic gecko foot-hair micro/nano-structures as dry adhesives. *J. Adhes. Sci. Technol.* **17**, 1055-1073.
Slifer, E. H. (1950). Vulnerable areas on the surface of the tarsus and pretarsus of the grasshopper (Acrididae, Orthoptera) with special reference to the arolium. *Ann. Entomol. Soc. Am.* **43**, 173-188.
Smith, C. W., Herbert, R., Wootton, R. J. and Evans, K. E. (2000). The hind wing of the desert locust (*Schistocerca gregaria* Forskal). II. Mechanical properties and functioning of the membrane. *J. Exp. Biol.* **203**, 2933-2943.
Snodgrass, R. E. (1935). *Principles of Insect Morphology*. New York: McGraw-Hill.
Spolenak, R., Gorb, S. and Arzt, E. (2005). Adhesion design maps for bio-inspired attachment systems. *Acta Biomater.* **1**, 5-13.
Stork, N. E. (1980a). Experimental analysis of adhesion of *Chrysolina polita* (Chrysomelidae: Coleoptera) on a variety of surfaces. *J. Exp. Biol.* **88**, 91-107.
Stork, N. E. (1980b). A scanning electron microscope study of tarsal adhesive setae in the Coleoptera. *Zool. J. Linn. Soc.* **68**, 173-306.
Stork, N. E. and Evans, E. G. (1976). Tarsal setae in Coleoptera. *Int. J. Insect Morphol. Embryol.* **5**, 219-221.
Taylor, A. M., Bonser, R. H. C. and Farrent, J. W. (2004). The influence of hydration on the tensile and compressive properties of avian keratinous tissues. *J. Mater. Sci.* **39**, 939-942.
Vincent, J. F. V. and Wegst, U. G. K. (2004). Design and mechanical properties of insect cuticle. *Arthropod. Struct. Dev.* **33**, 187-199.
Voigt, D., Schuppert, J. M., Dattinger, S. and Gorb, S. N. (2008). Sexual dimorphism in the attachment ability of the Colorado potato beetle *Leptinotarsa decemlineata* (Coleoptera: Chrysomelidae) to rough substrates. *J. Insect Physiol.* **54**, 765-776.
Yamaguchi, T., Gravish, N., Autumn, K. and Creton, C. (2009). Microscopic modeling of the dynamics of frictional adhesion in the gecko attachment system. *J. Phys. Chem. B.* **113**, 3622-3628.